

Rotating Solar Models with Low Metal Abundances as Good as Those with High Metal Abundances

Wuming Yang

Department of Astronomy, Beijing Normal University, Beijing 100875, China
 yangwuming@bnu.edu.cn, yangwuming@ynao.ac.cn

ABSTRACT

Standard solar models (SSM) constructed in accord with low metal abundances disagree with the seismically inferred results. We constructed rotating solar models with low metal abundances that included enhanced settling and convection overshoot. In one of our rotating models, **AGSSr2a**, the convection overshoot allowed us to recover the radius of the base of convection zone (CZ) at a level of 1σ . The rotational mixing almost completely counteracts the enhanced settling for the surface helium abundance, but only partially for the surface heavy-element abundance. At the level of 1σ , the combination of rotation and enhanced settling brings the surface helium abundance into agreement with the seismically inferred value of 0.2485 ± 0.0035 , and makes the model have better sound-speed and density profiles than SSM constructed in accordance with high metal abundances. The radius of the base of the CZ and the surface helium abundance of **AGSSr2a** are $0.713 R_{\odot}$ and 0.2472 , respectively; the absolute values of the relative differences in sound speed and density between it and the Sun are less than 0.0025 and 0.015 , respectively. Moreover, predicted neutrino fluxes of our model are comparable with the predictions of previous research works.

Subject headings: Sun: abundances — Sun: helioseismology — Sun: interiors — Sun: rotation

1. Introduction

The previously accepted value of the ratio of heavy-element abundance to hydrogen abundance of the Sun (Z/X), as derived from photospheric spectroscopy is 0.0244 (Grevesse & Noels 1993, hereafter GN93) or 0.0231 (Grevesse & Sauval 1998, hereafter GS98). Standard solar models (SSM) constructed in accordance with that ratio are thought to reproduce the seismically inferred results, such as the depth and helium abundance of the convection zone (CZ), and sound-speed and density profiles. The seismically inferred radius of the base of the CZ (BCZ) is $0.713 \pm 0.003 R_{\odot}$ (Christensen-Dalsgaard et al. 1991) or $0.713 \pm 0.001 R_{\odot}$ (Basu & Antia 1997), the helium abundance in the solar envelope is 0.2485 ± 0.0035 (Basu & Antia 2004; Serenelli & Basu 2010), **and the surface heavy-element abundance is in the range of 0.006 – 0.011 (Vorontsov et al.**

2014) or in the range of 0.008 – 0.014 (Buldgen et al. 2017).

Lodders (2003) and Asplund et al. (2004) analyzed the solar photospheric abundances and found that the value of Z/X in the present-day photosphere is in the range of about 0.0177 – 0.0165 , which is significantly lower than was previously thought. SSMs constructed in accord with this low Z/X disagree with the earlier seismically inferred results (Basu & Antia 2004; Bahcall et al. 2004, 2005; Montalbán et al. 2004, 2006; Turck-Chièze et al. 2004; Guzik et al. 2005; Castro et al. 2007; Yang & Bi 2007).

Asplund et al. (2009), Lodders et al. (2009), and Caffau et al. (2010) reanalyzed the solar photospheric abundances and revised the heavy-element abundance to $Z = 0.0134$ and $Z/X = 0.0181$ (Asplund et al. 2009, hereafter AGSS09), $Z = 0.0141$ and $Z/X = 0.0191$ (Lodders et al. 2009), and $Z = 0.0154$ and $Z/X = 0.0211$

(Caffau et al. 2010). SSMs constructed in accordance with these new low metal abundances also do not completely agree with the seismically inferred results (Serenelli et al. 2009; Serenelli & Basu 2010; Serenelli et al. 2011; Guzik et al. 2010; Bi et al. 2011; Le Pennec et al. 2015) and the neutrino flux constraints (Bahcall & Pinsonneault 2004; Turck-Chièze et al. 2004, 2010, 2011; Turck-Chièze & Thoul 2012; Lopes & Turck-Chièze 2013, 2014; Yang 2016).

Recently, von Steiger & Zurbuchen (2016) have claimed that the lower limit of solar metallicity (Z_{\odot}) derived from in situ solar wind composition is 0.0196, which is significantly larger than those of AGSS09 and Caffau et al. (2010), but consistent with that of Anders & Grevesse (1989). This seems to aggravate the “solar modeling problem” (or “solar abundance problem”). Serenelli et al. (2016) and Vagnozzi et al. (2017) have shown that the abundances found by von Steiger & Zurbuchen (2016) do not solve the problem but rather aggravate the surface helium abundance. The “solar modeling problem” thus remains unsolved.

Asplund et al. (2004) suggested that increased diffusion and settling of helium and heavy elements might be able to reconcile the low- Z models with helioseismology. It has been found that enhanced settling can significantly improve sound-speed and density profiles, but the surface helium abundance becomes too low and the position of the BCZ too shallow (Basu & Antia 2004; Montalbán et al. 2004; Guzik et al. 2005; Yang & Bi 2007; Yang 2016).

The effects of rotation on solar models have been studied by many authors (Pinsonneault et al. 1989; Yang & Bi 2006, 2007; Turck-Chièze et al. 2010; Yang 2016), including the centrifugal effect and rotational mixing. The former is insignificant for slowly rotating stars, but even for slowly rotating stars, the latter plays an important role in shaping their internal structures. Rotational mixing changes the distribution of the mean molecular weight, so it can improve the sound-speed profile (Yang & Bi 2006).

Proffitt & Michaud (1991) showed that macroscopic turbulent mixing can inhibit the settling of helium by about 40%, but Thoul, Bahcall & Loeb (1994) did not consider the effects of rotational and turbulent mixing on the diffusion and set-

ling of either helium or heavy elements in their diffusion coefficients. Rotational mixing can partially counteract microscopic diffusion and gravitational settling; so to obtain the same surface helium abundance in a rotating solar model as in a non-rotating SSM, the rates of microscopic diffusion and gravitational settling of p -modes Bahcall & Loeb (1994) should be enhanced in the rotating model.

In this work, our aim is to construct a solar model with low metal abundances that is as good as the SSMs with high metal abundances, e.g. in good agreement with the seismically inferred results. The paper is organized as follows. The properties of different solar models are presented in Section 2, calculation results are shown in Section 3, and the results are discussed and summarized in Section 4.

2. Properties of Solar Models

We used the Yale Rotation Evolution Code (YREC) (Pinsonneault et al. 1989; Yang & Bi 2007) in its rotation and non-rotation configurations to compute solar models and the Guenther (1994) pulsation code to calculate non-adiabatic oscillation frequencies of p -modes. We used the OPAL EOS2005 tables (Rogers & Nayfonov 2002) and OPAL opacity tables (Iglesias & Rogers 1996) with GN93, GS98, and AGSS09 mixtures, but supplemented by the Ferguson et al. (2005) opacity tables at low temperature as reconstructed with the GN93, GS98, and AGSS09 mixtures. We computed the diffusion and settling of both helium and heavy elements by using the formulas of Thoul, Bahcall & Loeb (1994); and we calculated the nuclear reaction rates by using the subroutine of Bahcall & Pinsonneault (1992) and Bahcall et al. (1995, 2001), but updated by the reaction data in Adelberger et al. (1998), Gruzinov & Bahcall (1998), and Marcucci et al. (2000). Convection was determined by the Schwarzschild criterion and treated according to the standard mixing-length theory. The depth of convection overshoot region was determined by $\delta_{\text{ov}}H_p$, where δ_{ov} is a free parameter and H_p is the local pressure scale height. Throughout much of the overshoot region, motion is no doubt sufficiently rapid to maintain the temperature gradient essentially at the adiabatic value

(Christensen-Dalsgaard et al. 1991). Thus, the overshoot region is assumed to be both fully mixed and adiabatically stratified.

All models are calibrated to the present solar luminosity 3.844×10^{33} erg s⁻¹, radius 6.9598×10^{10} cm, mass 1.9891×10^{33} g, and age 4.57 Gyr. The initial hydrogen abundance X_0 , metallicity Z_0 , and mixing-length parameter α are free parameters adjusted to match the constraints of luminosity and radius within around 10^{-5} **and an observed** $(Z/X)_s$. The initial rotation rate (Ω_i) of our rotating models is also a free parameter but adjusted to obtain a surface equatorial velocity of about 2.0 km s⁻¹ at the age of 4.57 Gyr. The distribution of the initial angular velocity is assumed to be uniform, and angular-momentum loss from the CZ due to magnetic braking is computed by using Kawaler’s relation (Kawaler 1988; Chaboyer et al 1995). The values of the parameters are summarized in Table 1.

In the rotating models, the redistributions of angular momentum and chemical compositions are treated as a diffusion process, i.e.

$$\frac{\partial \Omega}{\partial t} = f_\Omega \frac{1}{\rho r^4} \frac{\partial}{\partial r} (\rho r^4 D \frac{\partial \Omega}{\partial r}) \quad (1)$$

for the transport of angular momentum and

$$\begin{aligned} \frac{\partial X_i}{\partial t} = & f_c f_\Omega \frac{1}{\rho r^2} \frac{\partial}{\partial r} (\rho r^2 D \frac{\partial X_i}{\partial r}) \\ & + (\frac{\partial X_i}{\partial t})_{\text{nuc}} - \frac{1}{\rho r^2} \frac{\partial}{\partial r} (f_0 \rho r^2 X_i V_i) \end{aligned} \quad (2)$$

for the change in the mass fraction X_i of chemical species i , where D is the diffusion coefficient caused by rotational instabilities. Those instabilities include the Eddington circulation, the Goldreich-Schubert-Fricke instability (Pinsonneault et al. 1989), and the secular shear instability (Zahn 1993). In our calculations, the values of f_Ω and f_c are 1 and 0.03, respectively, though the value of f_c is commonly put at about 0.02 – 0.05 (Chaboyer & Zahn 1992; Yang & Bi 2006; Brott et al. 2011) to explain solar lithium depletion (Pinsonneault et al. 1989) and the extended main-sequence turnoffs in the color-magnitude diagram of intermediate-age massive star clusters in the Large Magellanic Cloud (Yang et al. 2013). The inhibiting effect of chemical gradients on the efficiency of rotational mixing is taken into consideration in our models and is regulated by the parameter f_μ with a value of 0.1 as described in

Pinsonneault et al. (1989). The second term on the **right-hand side** of Equation (2) represents the change caused by the nuclear reaction. In that equation, V_i is the velocity of microscopic diffusion and settling given by Thoul, Bahcall & Loeb (1994); and ρ is density. The parameter f_0 is a constant. In standard cases, the value of f_0 is equal to 1; but in an enhanced settling model, it is larger than 1. Moreover, in our rotating models, a convection overshoot of $\delta_{ov} = 0.1$ is required to reproduce the seismically inferred depth of the CZ.

3. Calculation Results

3.1. Solar models with high metal abundances

3.1.1. Standard solar models with high metal abundances

We first constructed two SSMs with high metal abundances — GN93M and GS98M — by using GN93 mixture opacities and GS98 mixture opacities, respectively. The radius r_{cz} of BCZ, the surface helium abundance Y_s , and other fundamental parameters of the models are shown in Table 1; and predicted and detected solar neutrino fluxes in Table 2. We compared the neutrino fluxes computed from our models with those calculated from the models BP04 (Bahcall & Pinsonneault 2004) and SSeM (Couvidat et al. 2003).

The sound speed and density of our models were compared with those inferred by Basu et al. (2009) using the data from the Birmingham Solar-Oscillations Network (Chaplin et al. 1996) and the Michelson Doppler Imager (Schou et al. 1998) (see Figure 1). The absolute values of relative sound-speed difference, $\delta c/c$, and density difference, $\delta \rho/\rho$, between the two SSMs and the Sun are less than 0.0041 and 0.027, respectively.

Figure 2 shows that the ratios of small to large separations, r_{02} and r_{13} , of our SSMs agree with those calculated from observed frequencies of Chaplin et al. (1999) or García et al. (2011). The neutrino fluxes computed from GS98M are comparable with those calculated from BP04 (Bahcall & Pinsonneault 2004) and those detected by Ahmed et al. (2004) and Bellini et al. (2011, 2012) (see Table 2). Therefore, we chose GS98M as our best SSM with high metal abundances and

went **on** to construct solar models with low metal abundances and compare them with this high abundance model.

3.1.2. *Enhanced diffusion and rotating models with high metal abundances*

We first needed to study the counteraction between rotational mixing and the diffusion of elements; so we constructed three enhanced settling models GS98x1, GS98x2, and GS98x3 and two rotating models GS98r1 and GS98r2. We enhanced the rates of element diffusion and settling in the first three models and in GS98r2 by applying a straight multiplier (f_0) to the diffusion velocity of Thoul, Bahcall & Loeb (1994), as Basu & Antia (2004), Montalbán et al. (2004), Guzik et al. (2005), and Yang & Bi (2007) **have done**, despite the fact that there is no obvious physical justification for such multiplier (Basu & Antia 2004; Guzik et al. 2005). For GS98x1, we increased the rates of element diffusion and settling by 10%, which did not affect its properties except for the surface helium abundance (see Figure 1 and Table 1). For GS98x2, we enhanced the rates by 50%. This significantly improved its sound-speed and density profiles (see Figure 1), but led to the fact that its surface helium abundance is too low. Moreover, the multiplier is too large. The theoretical error of the gravitational settling rate is of the order of about 15% (Thoul, Bahcall & Loeb 1994) in cases that rotational and turbulent mixing is neglected. For GS98x3, we increased the rates by 100%; but we found that the surface helium abundance, **radius** r_{cz} , sound-speed and density profiles of GS98x3 become worse than those of GS98M and GS98x2. This implies that it is unlikely that the rates can be increased by 100%.

The effects of rotation can improve sound-speed and density profiles (Yang & Bi 2006). The profiles of rotating model GS98r1 is better than those of our best SSM with high metal abundance, GS98M. However, rotational mixing raised the surface helium abundance of GS98r1 to 0.2548, which is higher than the seismically inferred value of 0.2485 ± 0.0035 . In order to reconcile the high surface helium abundance with that inferred, we needed to enhance the rates of element diffusion and settling in the rotating model.

We enhanced the rates of element diffusion and

settling of rotating model GS98r2 by 50% as high as that of enhanced settling model GS98x2 mentioned above. The absolute values of the relative sound-speed and density differences between GS98r2 and the Sun were found to be less than **0.003** and **0.0155**, respectively, which is better than those of GS98M (see Figure 1). The predicted neutrino fluxes of GS98r2 are almost the same as those of GS98M; but the surface helium abundance of **0.2466** for GS98r2 is larger than the 0.2315 of GS98x2, though smaller than the 0.2548 of GS98r1.

The initial helium abundances of GS98M, GS98x2, GS98r1, and GS98r2 were 0.27669, **0.27635**, 0.27518, and **0.27590**, respectively. Gravitational settling reduced the surface helium abundance of GS98M by about 11.7% below its initial value, and that of GS98x2, GS98r1, and GS98r2 by around **15.5%**, 7.4%, and **10.6%**, respectively. Figure 3 shows the distributions of helium abundances of the models as a function of radius. Due to the enhanced settling, the central helium abundance of GS98x2 was higher than that of GS98M, but its surface helium abundance lower. Rotational mixing made the surface helium abundance of GS98r1 higher than that of GS98M. In GS98r2, the effect of rotational mixing on the surface helium abundance was almost counteracted by the increased settling. Thus its surface helium abundance is almost consistent with that of GS98M. This implies that the velocity of element diffusion and settling should be increased by roughly 50% to obtain the same surface helium abundance in a rotating solar model as in a non-rotating SSM.

3.2. **Solar models with low metal abundances**

3.2.1. *Standard and enhanced diffusion models*

The SSM AGSS1 constructed with AGSS09 mixture opacities disagrees with the seismically inferred results, as has generally been found. In order to study the effects of enhanced settling, we constructed two models with low metal abundances — AGSSx2 and AGSSx3 — with different multipliers (see Table 1). **Models AGSSx2 and AGSSx3 had the Z/X determined by Lodders et al. (2009). The enhanced settling required a high Z_0 to reproduce the**

observed Z/X . The sound-speed and density profiles of AGSSx2 and AGSSx3 are obviously better than those of **AGSS1** (see Figure 4). This implies that enhanced settling aids in improving solar models. **We also constructed a model AGSSx2a with the surface heavy-element abundance determined by Caffau et al. (2010).** The sound-speed and density profiles of AGSSx2a are better than those of AGSSx2, even better than those of GS98M (see Figure 4). This can be partially attributed to the increased settling and the initial metal abundance. The value of Z_0 of **AGSSx2a** is larger than that of **AGSSx2**. The inferred sound speed and density are more easily reproduced by a model with a high initial metal abundance. The enhanced settling results in the main differences between **AGSS1** and **AGSSx2**. **But the higher Z_0 of AGSSx2a leads to the differences between AGSSx2 and AGSSx2a.**

However, Table 1 shows that the larger the value of f_0 , the lower the surface helium abundance. The surface helium abundances of AGSSx2, **AGSSx2a**, and AGSSx3 are lower than the seismically inferred value. Moreover, Figures 2 and 5 show that the r_{02} and r_{13} of the enhanced settling models deviate from the observed ones with an increase in the multiplier. Only the r_{02} and r_{13} of AGSSx2 and **AGSSx2a** whose diffusion velocities are enhanced by 50% agree with the observed ones. This indicates that, as has been found by Basu & Antia (2004), Guzik et al. (2005), and Yang (2016), enhanced settling alone cannot solve the solar modeling problem.

3.2.2. Rotating models as good as GS98M

Considering that rotational mixing can counteract enhanced settling to a certain degree, we constructed **three** rotating models — AGSSr2, **AGSSr2a**, and AGSSr3 — with AGSS09 mixture opacities. **Models AGSSr2 and AGSSr3 had the surface heavy-element abundance derived by Lodders et al. (2009), but AGSSr2a had that determined by Caffau et al. (2010).** Table 1 lists their fundamental parameters. Figure 6 shows that AGSSr3 has a better density profile, but it cannot reproduce the observed r_{02} and r_{13} (see Figure 7) and the seismically inferred surface helium abundance (see Table 1). This is due to the fact that the enhanced settling is too large

to be counteracted by rotational mixing. Thus AGSSr3 is not a good solar model.

The radius r_{cz} , sound-speed and density profiles of AGSSr2 are as good as those of GS98M (see Table 1 and Figure 6). It also reproduces the observed r_{02} and r_{13} (see Figure 7). Moreover, the neutrino fluxes computed from AGSSr2 are more consistent with the detected ones than other models (see Table 2). However, its surface helium abundance of 0.2425 is slightly lower than the seismically inferred value of 0.2485 ± 0.035 .

Table 1 shows that **AGSSr2a** reproduces the seismically inferred surface helium abundance and the radius r_{cz} at the level of 1σ . It also reproduces the observed r_{02} and r_{13} (see Figure 7). Furthermore, **AGSSr2a** has better sound-speed and density profiles than GS98M (see Figure 6). The absolute values of $\delta c/c$ and $\delta\rho/\rho$ between **AGSSr2a** and the Sun are less than 0.0025 and 0.015, respectively. Predicted neutrino fluxes of **AGSSr2a** are comparable with the predictions of BP04 and GS98M and the detected values (see Table 2). The surface metallicity of $Z = 0.0152$ is higher than that determined by AGSS09, but is in good agreement with the value of 0.0154 estimated by Caffau et al. (2010). **AGSSr2a** is thus a solar model as good as, and to a certain degree even better than, our best model with high metal abundance, GS98M. It has better sound-speed and density profiles, and its surface helium abundance of 0.2472 is in good agreement with 0.2485 ± 0.0035 . Moreover, the radius of the BCZ of **AGSSr2a** — $0.713 R_\odot$ — is also consistent with the seismically inferred value of $0.713 \pm 0.001 R_\odot$ (Basu & Antia 1997). Therefore, we chose **AGSSr2a** as our overall best model. This rotating solar model with low metal abundances is comparable to, or even slightly better than the SSMs with high metal abundances.

Gravitational settling reduces the surface helium abundance by about 11.7% in GS98M and around 10.8% in **AGSSr2a** below their initial values, which shows that for the surface helium abundance the enhanced settling was counteracted by rotational mixing. Therefore, at the level of 1σ the surface helium abundance of **AGSSr2a** is in agreement with the seismically inferred value. Moreover, the gravitational settling reduces the

heavy-element abundance in the CZ by around 10.1% in GS98M, 14.5% in **AGSSx2a**, and 13.8% in **AGSSr2a** below their initial values. For heavy elements, the enhanced settling is only partially counteracted by rotational mixing, which, as Equation (2) shows, is dependent on the radial gradient of elements. Due to the fact that central hydrogen burning is continuously producing helium, the gradient of helium abundance in the Sun arises from gravitational settling along with central hydrogen burning. However, the gradient of heavy elements results only from gravitational settling. Even in the radiative region with $r \gtrsim 0.2 R_{\odot}$, the gradient of helium abundance is markedly larger than that of the heavy elements (see Figure 8), which leads to the fact that the effect of rotational mixing on helium abundance is larger than that on heavy-element abundance. In other words, rotational mixing can more efficiently inhibit the settling of helium than of heavy elements. As a consequence, in the rotating model — **AGSSr2a**, the effect of the enhanced settling on the surface helium abundance is almost counteracted by rotational mixing, but that effect on the heavy-element abundance in the CZ is only partially offset by the mixing. This leads to the fact that the surface helium abundance of **AGSSr2a** is almost the same as that of GS98M, but the heavy-element abundance in the CZ of **AGSSr2a** is lower.

3.2.3. Internal rotations of models

Figure 8 shows the distributions of the diffusion coefficient D of rotational instabilities, angular velocity, helium abundance, and metal abundance of model **AGSSr2a** at different ages as a function of radius. The large gradient of angular velocity at around $r = 0.2 R_{\odot}$ leads to an increase in D (see panels *a* and *b* of Figure 8). The diffusion coefficient D is dependent on evolutionary states. The central angular velocity is about 5 times as large as the surface angular velocity. Seismically inferred results show that the solar angular velocity profile is flat in the radiative region of the Sun (Chaplin et al. 1999a). The internal rotation rate of **AGSSr2a** is higher than that of the Sun and its total angular momentum is about $3.97 \times 10^{48} \text{ g cm}^2 \text{ s}^{-1}$, which is larger than that of the Sun as inferred by Komm et al. (2003): $(1.94 \pm 0.05) \times 10^{48} \text{ g cm}^2 \text{ s}^{-1}$. A decrease in the initial angular velocity cannot bring the total angular momentum into

agreement with the seismically inferred one. For example, the initial angular velocity of GS98r1 is lower than that of **AGSSr2a**; and the total angular momentum of GS98r1 is $3.86 \times 10^{48} \text{ g cm}^2 \text{ s}^{-1}$.

The instabilities considered in this work mainly take effect in the region with $r \gtrsim 0.2 R_{\odot}$. The core contracts as the Sun evolves and so rotates faster and faster. These lead to too high internal angular velocities in the rotating models and a total angular momentum that is larger than the seismically inferred one. This indicates that there must be a mechanism of angular momentum transport affecting the inner layers of the models' radiative region. But it is missing. A gravity wave (Charbonnel & Talon 2005; García et al. 2007) or other mechanism (Denissenkov et al. 2008) might be a candidate for the angular momentum transport in these layers. **Such additional angular-momentum transport would obviously change the evolution of the internal rotation rate and hence the effects of turbulent diffusion on the composition.**

4. Discussion and Summary

A convection overshoot is required in rotating models to match the inferred depth of the CZ; but it is not required in the increased settling models, **AGSSx2a** and **AGSSx3**. This is partially due to the initial element abundances and rotational mixing, which lead to rotating models having different distributions of elements. **An increased settling requires a higher Z_0 .** The seismically inferred sound speed and depth of the CZ are more easily reproduced by a model with a higher metallicity. The enhanced settling model, **AGSSx2a**, has a higher Z_0 . **For **AGSSx2**, a convection overshoot of $\delta_{\text{ov}} = 0.1$ is required to match the inferred depth of the CZ.**

In our models, rotational mixing plays a major role in recovering the surface helium abundance and sound-speed profile. The mixing is dependent on the diffusion coefficient D of rotational instabilities, including those described by Pinsonneault et al. (1989), and the secular shear instability of Zahn (1993). The occurrence of rotational instabilities is thought to be related to the critical Reynolds number R_{crit} , the value of which in our calculations is 1000, in line with the default

of Endal & Sofia (1978) and Pinsonneault et al. (1989). The diffusion coefficient D is dependent on the evolutionary states. Different scenarios for the evolution of rotation could lead to different turbulent diffusion **to a certain degree, and hence also the turbulent diffusion and composition profiles.**

According to the works of Chaboyer & Zahn (1992) and Maeder & Zahn (1998), angular momentum is transported through advection (by meridional circulation velocity \mathbf{u}) and through turbulent diffusion; but the vertical transport of chemical elements can still be described by a diffusion equation. The advection term in the equation of angular momentum transport of Maeder & Zahn (1998) is not considered in the YREC. The effect of Eddington circulation on the redistribution of angular momentum is treated as a diffusion process in the YREC. This could affect the angular velocity profiles of our models to a certain degree.

Yang & Bi (2007), Turck-Chièze et al. (2010), and Yang (2016) studied the effects of rotation on solar models and found that the effects of rotation alone cannot solve the solar modeling problem. A combination of rotation and increased settling is required in our models to explain both the low-metal abundance and the seismically inferred results. The values of multiplier (f_0) in Yang & Bi (2007) and Yang (2016) are greater than or equal to 2. In that case, rotational mixing cannot counteract the increased settling, not even for the surface helium abundance. Different from the earlier models of Yang & Bi (2007) and Yang (2016), in **AGSSr2a**, in which the multiplier is 1.5, rotational mixing almost completely counteracts the effect of the increased settling for its surface helium abundance. The sound-speed profile, surface helium abundance, depth of the CZ, and r_{02} and r_{13} of **AGSSr2a** are thus in better agreement with seismically inferred ones than those of the earlier models, and the neutrino fluxes computed from **AGSSr2a** are more consistent with those detected by Ahmed et al. (2004) and Bellini et al. (2011, 2012) and predictions of BP04 (Bahcall & Pinsonneault 2004) than those calculated from the earlier models. Therefore, **AGSSr2a** is significantly better than the earlier models.

However, there is no obvious physical justifi-

cation for the multiplier. Rotational mixing can partially counteract the microscopic diffusion and gravitational settling. Therefore, in order to obtain the same surface helium abundance in a rotating solar model as in a non-rotating SSM, the rates of microscopic diffusion and gravitational settling need to be enhanced in the rotating model.

Convection overshoot also can lead to an increase in the surface helium abundance (Montalbán et al. 2006; Castro et al. 2007). But comparing with the effect of rotational mixing, Yang (2016) shows that the effect of a convection overshoot of $\delta_{ov} = 0.1$ on the surface helium abundance is negligible. The main effect of the overshoot is to bring the depth of the CZ into agreement with the seismically inferred one. If the overshoot is not considered in rotating models, the depth of the CZ of the models will be too shallow.

In our calculations, we computed the nuclear reaction rates by using the subroutine of Bahcall & Pinsonneault (1992), but updated by Bahcall et al. (1995) and Bahcall et al. (2001) using new reaction data. The discrepancy between the *hep* neutrino flux of our models and that of BP04 can be attributed to the nuclear cross section factor $S_0(\text{hep})$ (Bahcall et al. 2001). We used the factor of Marcucci et al. (2000) for *hep* neutrino flux, which affects only the flux of *hep* neutrinos, not those of other neutrinos (Yang 2016). The factors of nuclear reaction cross sections could affect the predicted neutrino fluxes and lead to the fact that the neutrino fluxes of our models are more consistent with those of BP04 (Bahcall & Pinsonneault 2004) rather than those of SSeM (Turck-Chièze & Couvidat 2011). The ${}^7\text{Be}$ neutrino fluxes predicted by **GS98M** and **AGSSr2a** agree with the detected one and the prediction of BP04 at the level of 2σ ; and the fluxes of *pp*, *pep*, ${}^8\text{B}$, ${}^{13}\text{N}$, ${}^{15}\text{O}$, and ${}^{17}\text{F}$ neutrinos computed from **AGSSr2a** are in good agreement with the predictions of BP04.

If the surface metallicity of SSM with GS98 mixtures is increased to 0.01809, we can obtain model GS98Ma with $r_{cz} = 0.715 R_\odot$ and $Y_s = 0.2483$, and with absolute values of $\delta c/c$ and $\delta\rho/\rho$ that are less than 0.0033 and 0.020, respectively. The neutrino fluxes predicted by GS98Ma are almost the same as the predictions of **AGSSr2a**, but **AGSSr2a** has better sound-speed and density profiles than GS98Ma (see **Figure 6**). Thus

AGSSr2a is better than GS98Ma and is still the best model in our calculations.

In this work, we constructed rotating solar models with the AGSS09 mixture opacities where the effects of enhanced settling and convection overshoot were included. We obtained a rotating model **AGSSr2a** that is better than SSM GS98M and the earlier rotating models of Yang & Bi (2007) and Yang (2016). The surface helium abundance of **AGSSr2a** is 0.2472, which agrees with the seismically inferred value at the level of 1σ . The radius of the BCZ of $0.713 R_{\odot}$ is also consistent with the seismically inferred value of $0.713 \pm 0.001 R_{\odot}$ (Basu & Antia 1997). The absolute values of $\delta c/c$ and $\delta\rho/\rho$ are less than 0.0025 and 0.015 for **AGSSr2a**, respectively. The sound speed and density of **AGSSr2a** are more consistent with the seismically inferred values (Basu et al. 2009) than those of GS98M. The surface metal abundance of **AGSSr2a** is 0.0152, which is higher than the value evaluated by AGSS09, but in agreement with the 0.0154 determined by Caffau et al. (2010). The initial helium abundance of **AGSSr2a** is 0.27721, which is consistent with the value of 0.273 ± 0.006 inferred by Serenelli & Basu (2010).

The main effect of convection overshoot is to bring the radius of the BCZ into agreement with the seismically inferred value at the level of 1σ . In the model, the velocities of diffusion and settling of helium and heavy elements of Thoul, Bahcall & Loeb (1994) are enhanced by 50%. Rotational mixing almost completely counteracts the increased settling for the surface helium abundance, but only partially for the heavy-element abundance in the CZ. As a consequence, the surface helium abundance of **AGSSr2a** is almost as high as that of GS98M, but the surface heavy-element abundance is lower. A combination of the enhanced settling and the effects of rotation allows us to recover the surface helium abundance at the level of 1σ and makes the model have better sound-speed and density profiles than GS98M. The effects of rotation should not be neglected in solar models. However, the internal angular velocity and total angular momentum of the rotating model are higher than the seismically inferred values. A mechanism mainly taking effect in inner layers of models' radiative region is needed to solve the fast rotation problem.

The author thanks the anonymous referee for helpful comments that helped the author improve this work and Daniel Kister for help in improving the English, and also acknowledges support from the NSFC 11773005 and U1631236.

REFERENCES

- Adelberger, E. C., Austin, S. M., Bahcall, J. N. et al. 1998, *Rev. Mod. Phys.*, 70, 1265
- Ahmed, S. N., Anthony, A. E., Beier, E. W. et al. 2004, *PhRvL*, 92, 1301
- Anders, E., & Grevesse, N. 1989, *GeCoA*, 53, 197
- Asplund, M., Grevesse N., Sauval, A. J., Allende Prieto, C., & Kiselman, D. 2004, *A&A*, 417, 751
- Asplund, M., Grevesse, N., Sauval, A., & Scott, P. 2009, *ARA&A*, 47, 481 (AGSS09)
- Bahcall, J. N., Pinsonneault, M. H., & Basu, S, 2001, *ApJ*, 555, 990
- Bahcall, J. N., & Pinsonneault, M. H. 1992, *Rev. Mod. Phys.*, 64, 885
- Bahcall J. N., Pinsonneault M. H., & Wasserburg G. J. 1995, *Rev. Mod. Phys.*, 67, 781
- Bahcall, J. N., & Pinsonneault, M. H. 2004, *Phys. Rev. Lett.*, 92, 121301
- Bahcall, J. N., Serenelli, A. M., & Pinsonneault, M. H. 2004, *ApJ*, 614,464
- Bahcall, J. N., Basu, S., Pinsonneault, M. H., & Serenelli, A. M. 2005, *ApJ*, 618, 1049
- Basu, S., & Antia, H. M. 1997, *MNRAS*, 287, 189
- Basu, S., Chaplin, W. J., Elsworth, Y., New, R., Serenelli, A. M. 2009, *ApJ*, 699, 1403
- Basu, S., & Antia, H. M. 2004, *ApJ*, 606, L85
- Bellini, G. Benziger, J. Bick, D. et al. 2011, *PhRvL*, 107, 141302
- Bellini, G. Benziger, J. Bick, D. et al. 2012, *PhRvL*, 108, 51302
- Bi, S. L., Li, T. D., Li, L. H., Yang, W. M. 2011, *ApJL*, 731, 42

- Brott, I., Evans, C. J., Hunter, I., et al. 2011, *A&A*, 530, A116
- Buldgen, G., Salmon, S. J. A. J., Noels, A., Scuflaire, R., Dupret, M. A., Reese, D. R. 2017, *MNRAS*, 472, 751
- Caffau, E., Ludwig, H.-G., Bonifacio, P., Faragiana, R., Steffen, M., Freytag, B., Kamp, I., Ayres, T. R. 2010, *A&A*, 514, A92
- Castro, M., Vauclair, S., Richard, O. 2007, *A&A*, 463, 755
- Chaboyer, B., Demarque, P., Pinsonneault, M. H. 1995, 441, 865
- Chaboyer, B., & Zahn, J. P. 1992, *A&A*, 253, 173
- Chaplin, W. J., Christensen-Dalsgaard, J., Elsworth, Y., et al. 1999a, *MNRAS*, 308, 405
- Chaplin, W. J., Elsworth, Y., Howe, R., et al. 1996, *Sol. Phys.*, 168, 1
- Chaplin, W. J., Elsworth, Y., Isaak, G. R., Miller, B. A., & New, R. 1999b, *MNRAS*, 308, 424
- Charbonnel, C., & Talon, S. 2005, *Science*, 309, 2189
- Christensen-Dalsgaard, J., Gough, D. O., & Thompson, M. J. 1991, *ApJ*, 378, 413
- Couvidat, S., Turck-Chièze, S., & Kosovichev, A. G. 2003, *ApJ*, 599, 1434
- Denissenkov, P. A., Pinsonneault, M., MacGregor, K. B. 2008, *ApJ*, 684, 757
- Endal, A. S., & Sofia, S. 1978, *ApJ*, 220, 279
- Ferguson, J. W., Alexander, D. R., Allard, F. et al. 2005, *ApJ*, 623, 585
- García, R. A., Salabert, D., & Ballot, J. et al., 2011, *JPhCS*, 271, 012049
- García, R. A., Turck-Chièze, S., Jiménez-Reyes, S. J., Ballot, J., Pallé, P. L., Eff-Darwich, A., Mathur, S., Provost, J. 2007, *Sci.*, 316, 1591
- Grevesse, N., Noels, A. 1993. In *Origin and Evolution of the Elements*, ed. N Prantzos, E Vangioni-Flam, MCassé, pp. 15 – 25. Cambridge, UK: Cambridge Univ. Press. 561 pp. (GN93)
- Grevesse, N., & Sauval, A. J. 1998, in *Solar Composition and Its Evolution*, ed. C. Fröhlich, et al. (Dordrecht: Kluwer), 161 (GS98)
- Gruzinov, A. V., & Bahcall, J. N. 1998, *ApJ*, 504, 996
- Guenther D. B., 1994, *ApJ*, 422, 400
- Guzik, J. A., Watson, L. S. & Cox, A. N. 2005, *ApJ*, 627, 1049
- Guzik, J. A., & Mussack, K. 2010, *ApJ*, 713, 1108
- Iglesias, C., Rogers, F. J. 1996, *ApJ*, 464, 943
- Kawaler, S. D. 1988, *ApJ*, 333, 236
- Komm, R., Howe, R., Durney, B. R., & Hill, F. 2003, *ApJ*, 586, 650
- Le Pennec, M., Turck-Chièze, S., Salmon, S., Blancard, C., Cossé, P., Faussurier, G., Mondet, G. 2015, *ApJL*, 813, L42
- Lodders, K. 2003, *ApJ*, 591, 1220
- Lodders, K, Palme, H, Gail, H-P. 2009, *LanB*, 4, 44
- Lopes, I., & Turck-Chièze, S. 2013, *ApJ*, 765, 14
- Lopes, I., & Turck-Chièze, S. 2014, *ApJL*, 792, L35
- Maeder, A., & Zahn, J.-P. 1998, *A&A*, 334, 1000
- Marcucci, L. E., Schiavilla, R., Viviani, M., Kievski, A., & Rosati, S. 2000, *Phys. Rev. Lett.*, 84, 5959
- Montalbán, J., Miglio, A., Noels, A., Grevesse, N., Di Mauro, M. P. 2004, in *Helio- and Asteroseismology: Towards a Golden Future*, Proc. of the SOHO 14 / GONG 2004 Workshop, ed. D. Danesy (ESA SP-559; Noordwijk: ESA), 574
- Montalban, J., Miglio, A., Theado, S., Noels, A., Grevesse, N. 2006, *Commun. Asteroseismol.*, 147, 80
- Pinsonneault, M. H., Kawaler, S. D., Sofia, S., & Demarque, P., 1989, *ApJ*, 338, 424
- Proffitt, C. R., & Michaud, G. 1991, *ApJ*, 380, 238
- Rogers, F., & Nayfonov, A. 2002, *ApJ*, 576, 1064

- Schou, J., Antia, H. M., Basu, S. et al. 1998, *ApJ*, 505, 390
- Serenelli, A., & Basu, S. 2010, *ApJ*, 719, 865
- Serenelli, A., Basu, S., Ferguson, J., & Asplund, M. 2009, *ApJL*, 705, 123
- Serenelli, A., Haxton, W. C., Peña-Garay, C. 2011, *ApJ*, 743, 24
- Serenelli, A. M., Scott, P., Villante, F. L., et al. 2016, *MNRAS*, 463, 2
- Thoul, A. A., Bahcall, J. N., Loeb, A. 1994, *ApJ*, 421, 828
- Turck-Chièze, S., & Couvidat, S. 2011, *RPPh*, 74, 6901
- Turck-Chièze, S., Couvidat, S., Piau, L., Ferguson, J., Lambert, P., Ballot, J., García, R. A., Nghiem, P. 2004, *Phys. Rev. Lett.*, 93, 211102
- Turck-Chièze, S., & Lopes, I. 2012, *RAA*, 12, 1107
- Turck-Chièze, S., Palacios, A., Marques, J. P., Nghiem, P. A. P. 2010, *ApJ*, 715, 1539
- Turck-Chièze, S., Piau, L., & Couvidat, S. 2011, *ApJL*, 731, L29
- Vagnozzi, S., Freese, K., Zurbuchen, T. H. 2017, *ApJ*, 839, 55
- von Steiger, R., & Zurbuchen, T. H. 2016, *ApJ*, 816, 13
- Vorontsov, S. V., Baturin, V. A., Ayukov, S. V., Gryaznov, V. K. 2014, *MNRAS*, 441, 3296
- Yang, W. M., & Bi, S. L. 2006, *A&A*, 449, 1161
- Yang, W. M., & Bi, S. L. 2007, *ApJ*, 658, L67
- Yang, W., Bi, S., Meng, X., & Liu, Z 2013, *ApJ*, 776, 112
- Yang, W. 2016, *ApJ*, 821, 108
- Zahn, J. P. 1993, in *Astrophysical Fluid Dynamics, Les Houches XLVII*, ed. J.-P. Zahn & Zinn-Justin (New York: Elsevier), 561

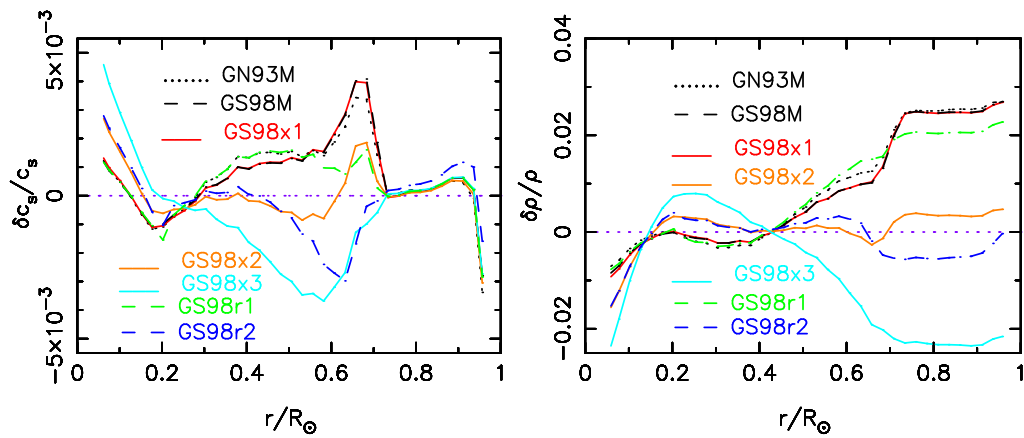


Fig. 1.— The relative sound-speed and density differences, in the sense of the (Sun-Model)/Model, between solar models and seismically inferred results. The seismically inferred sound speed and density are given in Basu et al. (2009). **The red line coincides with the black dashed line.**

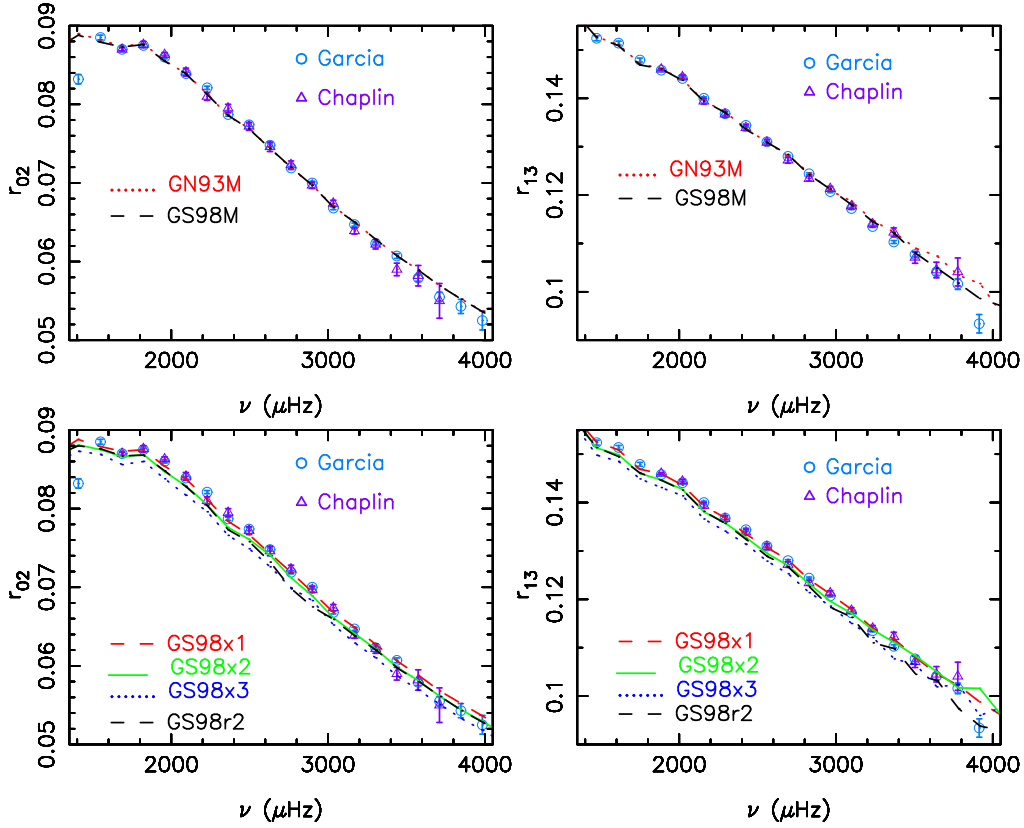


Fig. 2.— The distributions of the ratios of small to large separations, r_{02} and r_{13} , as a function of frequency. The circles and triangles show the ratios calculated from the frequencies observed by GOLF & VIRGO (García et al. 2011) and BiSON (Chaplin et al. 1999), respectively.

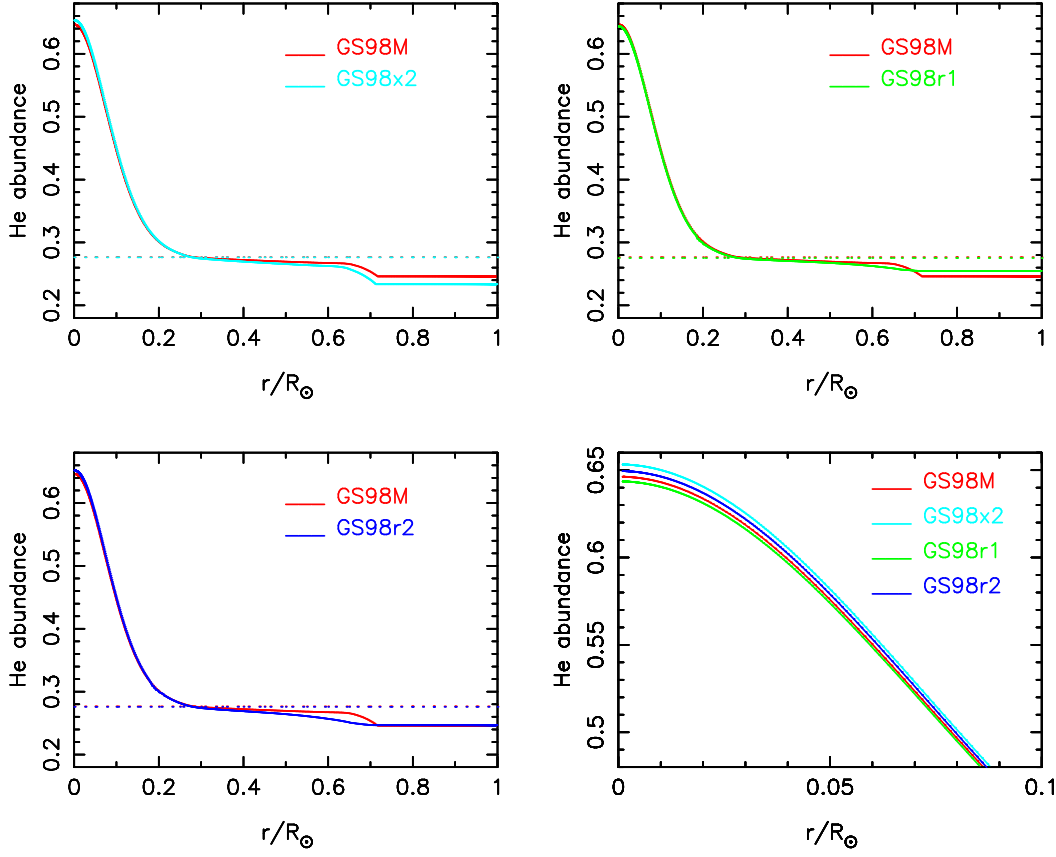


Fig. 3.— Distributions of He abundance of models as a function of radius. The dotted lines show the initial helium abundances of the models. The central He abundances of GS98x2 and GS98r2 are higher than that of GS98M, which is caused by the enhanced settling. The initial helium abundances of GS98M, GS98x2, GS98r1, and GS98r2 are **0.27669**, **0.27635**, **0.27518**, and **0.27590**, respectively.

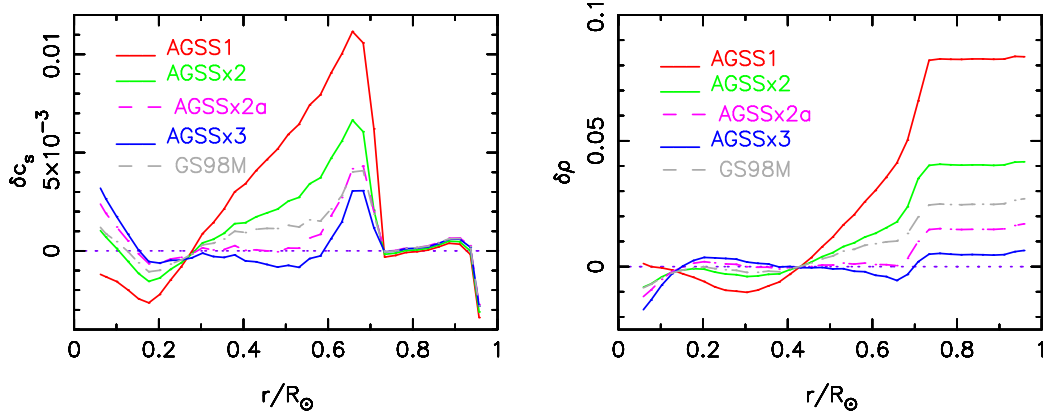


Fig. 4.— The relative sound-speed and density differences, in the sense of the (Sun-Model)/Model, between solar models and seismically inferred results. The seismically inferred sound speed and density are given in Basu et al. (2009).

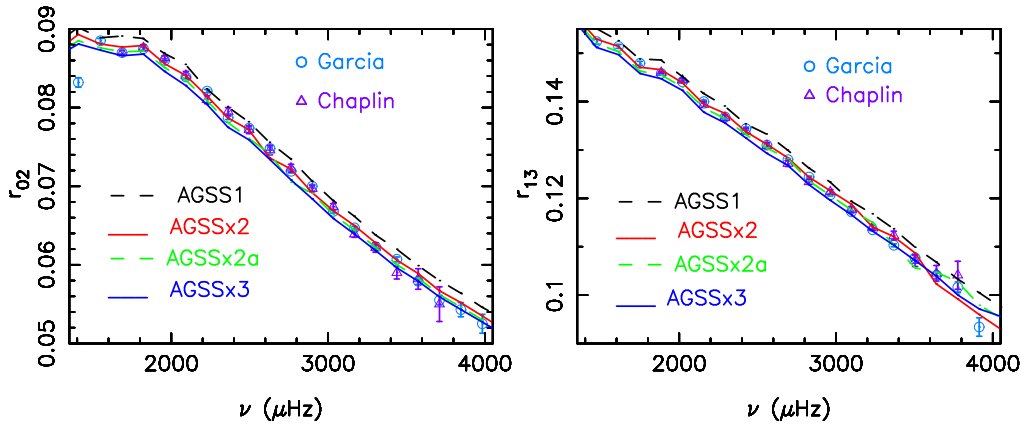


Fig. 5.— The distributions of the ratios of small to large separations, r_{02} and r_{13} , as a function of frequency. The circles and triangles show the ratios calculated from the frequencies observed by GOLF & VIRGO (García et al. 2011) and BiSON (Chaplin et al. 1999), respectively.

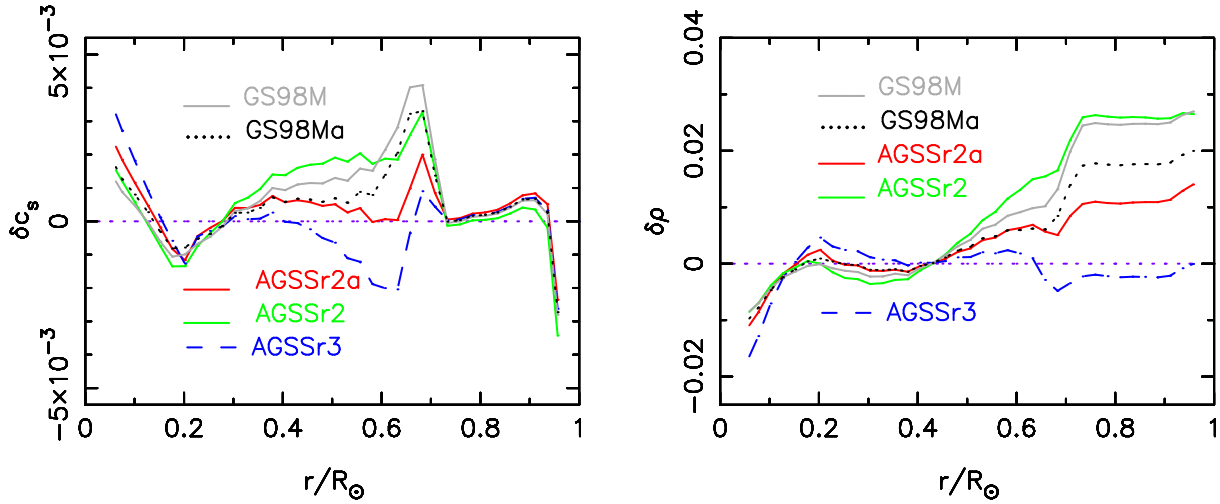


Fig. 6.— The relative sound-speed and density differences, in the sense of the (Sun-Model)/Model, between solar models and seismically inferred results. The seismically inferred sound speed and density are given in Basu et al. (2009).

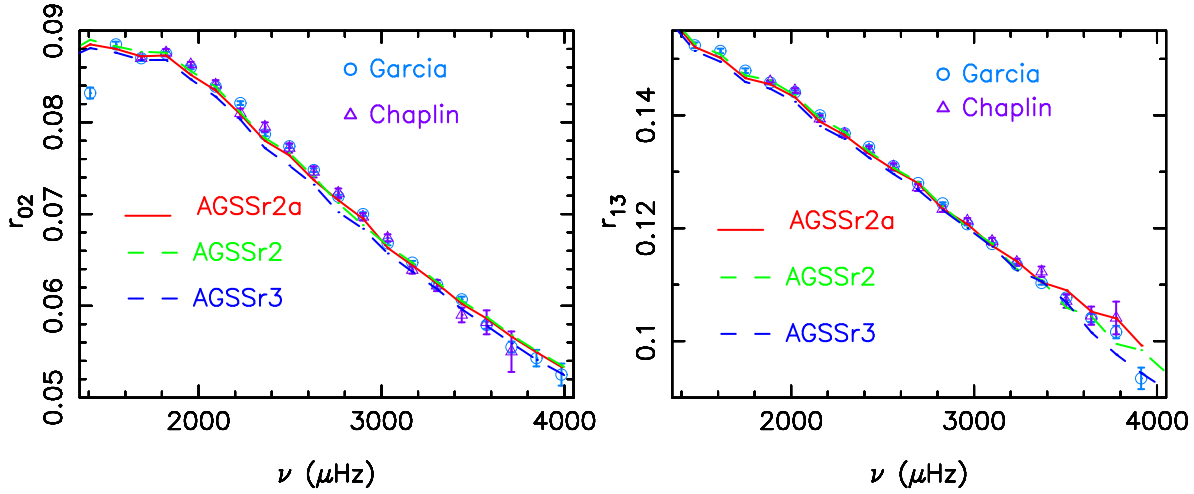


Fig. 7.— The distributions of the ratios of small to large separations, r_{02} and r_{13} , as a function of frequency. The circles and triangles show the ratios calculated from the frequencies observed by GOLF & VIRGO (García et al. 2011) and BiSON (Chaplin et al. 1999), respectively.

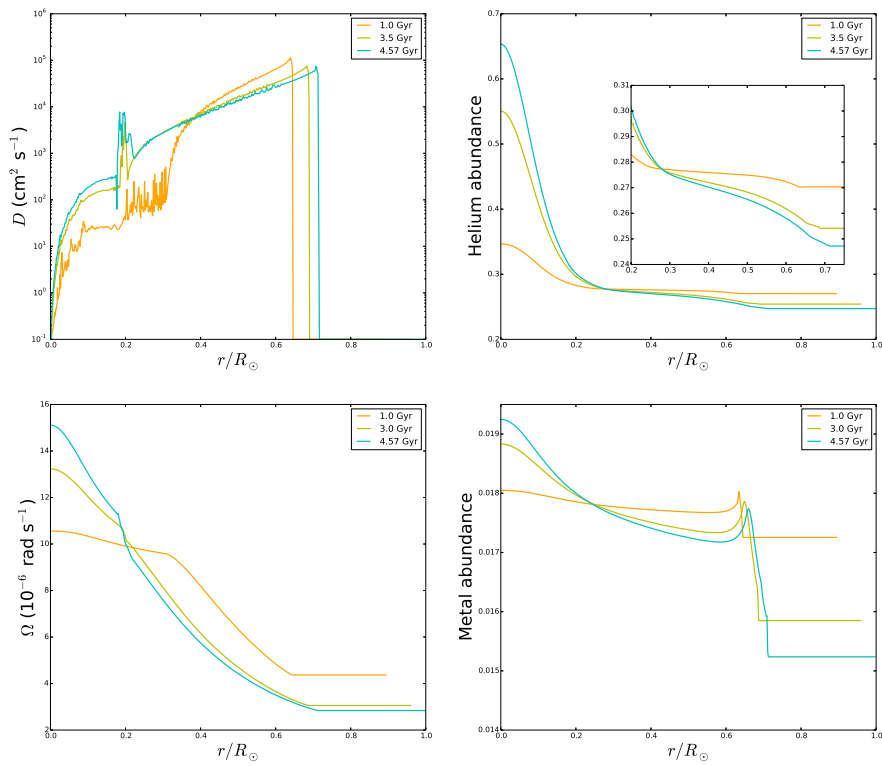


Fig. 8.— Distributions of diffusion coefficient D , angular velocity, helium abundance, and metal abundance of model **AGSSr2a** at different ages as a function of radius. The different color lines refer to different ages.

Table 1: Model parameters.

Model	X_0	Z_0	α	δ_{ov}	f_0	T_c	ρ_c	r_{cz} R_\odot	Y_s	Z_s	$(Z/X)_s$	Ω_i	V_e
GN93M	0.7061	0.02021	2.1130	0	1.0	1.576	154.41	0.715	0.2436	0.0182	0.0246	0	0
GS98M	0.7038	0.01950	2.1957	0	1.0	1.579	154.66	0.716	0.2461	0.0175	0.0238	0	0
GS98Ma	0.7010	0.02010	2.2130	0	1.0	1.583	155.05	0.715	0.2483	0.0181	0.0246	0	0
GS98x1	0.7051	0.01954	2.2365	0	1.1	1.579	154.82	0.716	0.2422	0.0174	0.0235	0	0
GS98x2	0.7038	0.01990	2.3110	0	1.5	1.587	156.35	0.712	0.2335	0.0171	0.0228	0	0
GS98x3	0.7014	0.02084	2.4730	0	2.0	1.598	158.40	0.707	0.2240	0.0171	0.0225	0	0
GS98r1	0.7056	0.01925	2.1665	0.1	1.0	1.576	154.34	0.712	0.2548	0.0174	0.0238	9.4	1.93
GS98r2	0.7045	0.01958	2.2392	0.1	1.5	1.584	156.16	0.710	0.2466	0.0168	0.0229	10	2.01
AGSS1	0.7179	0.01588	2.1801	0	1.0	1.564	152.04	0.727	0.2351	0.0142	0.0189	0	0
AGSSx2	0.7119	0.01686	2.3654	0.1	1.5	1.578	154.33	0.713	0.2283	0.0144	0.0191	0	0
AGSSx3	0.7068	0.01772	2.4585	0	2.0	1.593	156.60	0.715	0.2204	0.0145	0.0189	0	0
AGSSx2a	0.7022	0.01818	2.3577	0	1.5	1.592	155.51	0.716	0.2355	0.0155	0.0207	0	0
AGSSr2	0.7107	0.01700	2.3160	0.1	1.5	1.578	154.42	0.715	0.2425	0.0145	0.0196	10	1.99
AGSSr3	0.7090	0.01740	2.3890	0.1	2.0	1.588	156.31	0.712	0.2354	0.0142	0.0189	10	2.02
AGSSr2a	0.7050	0.01779	2.3098	0.1	1.5	1.586	155.13	0.713	0.2472	0.0152	0.0207	10	1.98

Notes. The central temperature T_c , central density ρ_c , initial angular velocity Ω_i , and surface equatorial velocity V_e are in unit of 10^7 K, g cm^{-3} , 10^{-6} rad s^{-1} , and km s^{-1} , respectively.

Table 2: Predicted solar neutrino fluxes from models.

model	pp	pep	hep	${}^7\text{Be}$	${}^8\text{B}$	${}^{13}\text{N}$	${}^{15}\text{O}$	${}^{17}\text{F}$
GN93M	5.95	1.40	9.51	5.03	5.10	5.77	5.05	5.59
GS98M	5.95	1.40	9.46	5.13	5.25	5.50	4.87	5.64
GS98Ma	5.93	1.40	9.40	5.23	5.47	5.85	5.21	6.04
GS98x1	5.95	1.40	9.47	5.12	5.23	5.51	4.87	5.65
GS98x2	5.92	1.39	9.36	5.31	5.67	6.10	5.45	6.34
GS98x3	5.87	1.38	9.21	5.59	6.35	7.17	6.49	7.59
GS98r1	5.95	1.40	9.46	5.00	5.00	5.26	4.63	5.35
GS98r2	5.92	1.40	9.34	5.21	5.47	5.88	5.23	6.08
AGSS1	6.01	1.43	9.77	4.70	4.38	3.88	3.36	3.86
AGSSx2	5.96	1.41	9.54	5.07	5.16	4.78	4.22	4.89
AGSSx3	5.91	1.39	9.33	5.45	6.03	5.82	5.23	6.11
AGSSx2a	5.91	1.39	9.31	5.43	5.99	5.80	5.22	6.08
AGSSr2	5.94	1.40	9.47	5.04	5.11	4.81	4.25	4.92
AGSSr3	5.90	1.39	9.34	5.28	5.66	5.47	4.89	5.70
AGSSr2a	5.92	1.39	9.34	5.25	5.60	5.42	4.84	5.62
BP04	5.94	1.40	7.88	4.86	5.79	5.71	5.03	5.91
SSeM	5.92	1.39	4.85	4.98	5.77	4.97	3.08
Measured	$6.06^{+0.02a}_{-0.06}$	1.6 ± 0.3^b	...	4.84 ± 0.24^a	$5.21\pm 0.27\pm 0.38^c$

Notes. The table shows the predicted fluxes, in units of $10^{10}(pp)$, $10^9({}^7\text{Be})$, $10^8(pep, {}^{13}\text{N}, {}^{15}\text{O})$, $10^6({}^8\text{B}, {}^{17}\text{F})$, and $10^3(hep)$ cm^2s^{-1} . The BP04 is the best model of Bahcall & Pinsonneault (2004) and has the GS98 mixtures. The SSeM is a standard model with high metal abundances that reproduces the seismic sound speed (Couvidat et al. 2003; Turck-Chièze & Couvidat 2011).

^aBellini et al. (2011).

^bBellini et al. (2012).

^cAhmed et al. (2004).